Global Change Biology (2007) **13**, 370–385, doi: 10.1111/j.1365-2486.2006.01298.x

A method for deriving net primary productivity and component respiratory fluxes from tower-based eddy covariance data: a case study using a 17-year data record from a Douglas-fir chronosequence

CHRISTOPHER R. SCHWALM*, T. ANDREW BLACK*, KAI MORGENSTERN* and ELYN R. HUMPHREYS†

Land and Food Systems, University of British Columbia, Vancouver, BC, Canada V6T 1Z4, †Department of Geography and Environmental Studies, Carleton University, Ottawa, ON, Canada K1S 5B6

Abstract

Conventional gap-filling procedures for eddy covariance (EC) data are limited to calculating ecosystem respiration (R_E) and gross ecosystem productivity (P_G) as well as missing values of net ecosystem productivity (F_{NEP}). We develop additional postprocessing steps that estimate net primary productivity (P_N), autotrophic (R_a), and heterotrophic respiration (R_h). This is based on conservation of mass of carbon (C), Monte Carlo (MC) simulation, and three ratios: C use efficiency (CUE, P_N to P_G), R_a to R_E, and F_{NEP} to R_E. This procedure, along with the estimation of F_{NEP}, R_E, and P_G, was applied to a Douglas-fir dominated chronosequence on Vancouver Island, British Columbia, Canada. The EC data set consists of 17 site years from three sites: initiation (HDF00), pole/sapling (HDF88), and near mature (DF49), with stand ages from 1 to 56 years. Analysis focuses on annual C flux totals and C balance ratios as a function of stand age, assuming a rotation age of 56 years. All six C balance terms generally increased with stand age. Average annual P_N by stand was 213, 750, and 1261 g C m^{-2} yr^{-1} for HDF00, HDF88, and DF49, respectively. The canopy compensation point, the year when the chronosequence switched from a source to a sink of C, occurred at stand age ca. 20 years. HDF00 and HDF88 were strong and moderate sources ($F_{NEP} = -581$ and -138 g C m^{-2} yr^{-1}), respectively, while DF49 was a moderate sink ($F_{NEP} = 294$ g C m^{-2} yr^{-1}) for C. Differences between sites were greater than interannual variation (IAV) within sites and highlighted the importance of age-related effects in C cycling. The validity of the approach is discussed using a sensitivity analysis, a comparison with growth and yield estimates from the same chronosequence, and an intercomparison with other chronosequences.

Keywords: autotrophic respiration, carbon use efficiency, chronosequence, Douglas-fir, eddy covariance, heterotrophic respiration, Monte Carlo simulation, net ecosystem productivity, net primary productivity, stand age

Received 23 May 2005; revised version received 31 August 2006 and accepted 8 October 2006

Introduction

Changes in carbon (C) cycling of forested ecosystems are related to succession (e.g. Kolari *et al.*, 2004). Microclimate (Chen *et al.*, 1993), the amount of coarse woody debris (Janisch & Harmon, 2002), leaf nitrogen (Gower *et al.*, 1996; Niinemets, 2002), and leaf area index (LAI, Waring & Schlesinger, 1985) all vary in predictable ways during succession. These changes affect C cycling via gross ecosystem productivity (P_G) or ecosystem respiration (R_E). Forested biomes consist of a mosaic of stand types along gradients of age, species composition, structural characteristics, and climate. Accurately determining the contribution of forested ecosystems to the global C budget must account for changes in net ecosystem productivity (F_{NEP}) over the course of stand development.

Correspondence: Christopher R. Schwalm, tel. +1 604 822 9119, fax +1 604 822 4400, e-mail: schw0516@umn.edu

© 2007 The Authors
Journal compilation © 2007 Blackwell Publishing Ltd

An important tool for investigating such relationships is tower-based eddy covariance (EC) installations (Baldocchi, 2003). There are currently over 360 EC stations used in terrestrial (primarily forested) biomes worldwide (http://www.fluxnet.ornl.gov/fluxnet/viewstatus.cfm). EC data, often in conjunction with chamber measurements (Drewitt *et al.*, 2002; Black *et al.*, 2004), are used to analyse the interdependencies between CO_2 and H_2O fluxes, C cycling, and environmental gradients. However, the long mean residence time of most forest vegetative assemblages makes EC measurements spanning seral stages or stages of stand development impractical. Most EC research sites are short term (Black *et al.*, 2004) with flux data spanning ca. 10 years available only at a small number of sites (e.g. Harvard Forest; Barford *et al.*, 2001). This difficulty in obtaining long-term data has led to the use of the chronosequence approach, whereby towers are placed in a cross-section of stands along an age gradient. Such stands are similar in terms of weather, stand type, and soil properties and allow the investigation of stand age–C balance relationships (e.g. Amiro, 2001; Anthoni *et al.*, 2002; Chen *et al.*, 2002, 2004; Litvak *et al.*, 2003; Humphreys *et al.*, 2006).

Despite the proliferation of chronosequence studies, EC-based research is limited in the extent the C budget is quantified. A temporally fine-scaled quantification of F_{NEP} is the sole C balance term measured by an EC system. However, when P_G is absent at night-time or in the dormant period F_{NEP} is assumed to equal $-R_E$. Statistical models of night-time R_E as a function of temperature are used to compute daytime R_E, which is assumed to follow the same temperature response as at night. P_G is then the sum of daytime R_E, a modelled quantity, and daytime F_{NEP}, a measured quantity. This procedure (Baldocchi *et al.*, 2001) has been used in numerous studies (e.g. Law *et al.*, 2002; Morgenstern *et al.*, 2004) but offers insight neither into the components of R_E nor net primary productivity (P_N).

The need to extrapolate beyond observed night-time temperatures complicates using the night-time R_E–temperature relationship in the daytime. This has led to studies that use soil, bole, and/or foliage chamber measurements to have a second independent assessment of R_E or its components. Quantifying either component of R_E would allow also calculation of the other and P_N by mass balance. However, chamber-based and EC-based measurements of R_E do not always agree (Lavigne *et al.*, 1997; Griffis *et al.*, 2004). Furthermore, soil chamber studies measure soil respiration (R_s), which must be separated into its autotrophic (R_a), and heterotrophic (R_h) components to calculate P_N. However, the controls on R_s are not well understood (Bond-Lamberty *et al.*, 2004a, b). This is partly due to the spatial variability in soil respiration that confounds efforts to arrive at a chamber-based measurement strictly comparable with an EC-based one (Drewitt *et al.*, 2002; Humphreys *et al.*, 2006). Methodological issues inhibit the development of robust quantitative relationships between soil respiration, its components, and explanatory variables (Bond-Lamberty *et al.*, 2004b). Variability and difficulty in measurement also confound efforts to accurately quantify and scale up autotrophic respiration (Williams *et al.*, 2005), specifically foliage and root respiration.

As another approach to quantify additional terms in the C balance, some researchers have combined EC data with C stock analysis (e.g. Law *et al.*, 2003; Harmon *et al.*, 2004) as a means to quantify P_N and its components concurrent with EC measurements. However, directly estimating P_N is difficult due to the uncertainties involved in measuring fine roots and exudates. Moreover, such efforts are rare, generally do not span a chronosequence, and are not temporally scaled in a uniform manner (Field & Kaduk, 2004; Harmon *et al.*, 2004). An EC system measures half-hourly fluxes, whereas C stock studies have coarser temporal resolutions, typically 1 year or greater. A uniform method to simultaneously estimate half-hourly F_{NEP}, R_E, P_G, P_N, R_a, and R_h (hereafter: C balance) does not currently exist.

This study examines the C balance in a chronosequence of three Douglas-fir (*Pseudotsuga menziesii*) dominated stands in coastal British Columbia. The EC data set consists of 17 site years with stand ages ranging from 1 to 56 years. Previous work in this chronosequence has focused on soil respiration (Drewitt *et al.*, 2002), environmental controls on interannual variation (IAV) and bias in annual C flux totals (Morgenstern *et al.*, 2004), variability in sensible and latent heat fluxes (Humphreys *et al.*, 2003), and the controls on daily and seasonal P_G, F_{NEP}, and R_E through 2003 (Humphreys *et al.*, 2005, 2006). This study augments previous work by tracking P_N, R_a, R_h, and C balance ratios (hereafter: efficiencies) through the life of the stand. Furthermore, six additional site years of data from 2004 and 2005 have been included. Specifically, the objective of this study is to estimate the C balance for the complete 17-year data set. P_N, R_a, and R_h are calculated from EC data using independent values of C use efficiency, mass balance of C, and Monte Carlo (MC) simulation. Statistical uncertainties for each flux are calculated using error propagation and bootstrapping. These estimates are then discussed in the context of establishing relationships between the C balance, efficiencies, and the stand age of Douglas-fir coastal forests. To facilitate discussion of longer-term trends, we estimate annual C balance values for missing years from a predictive model with stand age as the sole explanatory variable. A comparison of growth and yield output with annual P_N values,

© 2007 The Authors

as well as a sensitivity analysis to assess the inherent uncertainty of the MC-based procedure is then presented. Finally, we also contrast C balance–stand age relationships here with other chronosequences and discuss validation issues.

Materials and methods

Site characteristics

The chronosequence is located near Campbell River on Vancouver Island, BC, Canada in the coastal western hemlock (CWH) biogeoclimatic zone (Pojar *et al.*, 1991; MacKinnon, 2003). The CWH covers 3 million ha in coastal and insular BC, as well as parts of Alaska, Oregon, and Washington, USA. The chronosequence consists of three sites ranging from initiation to near mature stands, in terms of a typical rotation (Table 1), dominated by Douglas-fir. These differently aged stands represent secondary succession after logging, site preparation, and planting and have an expected rotation age of ca. 56 years (Spittlehouse, 2003). In modelling longer-term trends only interpolation between the end points of stand ages observed here will be discussed.

EC measurements and gap filling

The EC method was used to measure half-hourly F_{NEP} (μmol CO_2 m^{-2} ground area s^{-1}). This technique is based on high-frequency sampling of the turbulent motions of upward and downward moving CO_2 to determine the net flux moving across the canopy-atmosphere interface. This is accomplished by analysing the covariance of the vertical wind velocity and the CO_2 mixing ratio and assumes that this exchange is the sole mechanism by which CO_2 can enter or leave the ecosystem (Baldocchi, 2003). Despite continuous year-round operation of the EC towers, gaps occurred due to low turbulence at night-time, when friction velocity (u_*) was less than a critical threshold (Table 1), or sensor failure. Using only quality-controlled data a model between night-time R_E (=−night-time F_{NEP}) and soil temperature at 2 cm depth ($T_{s,2}$) was used to model gaps at night. This relationship was also applied to daytime F_{NEP} to estimate daytime R_E from the mass balance equation. P_G was similarly calculated: P_G = daytime F_{NEP} + daytime R_E. These steps (i.e. gap filling) followed Barr *et al.* (2004) with three modifications. (i) Instead of a logistic relationship between R_E and $T_{s,2}$ a linear relationship between log[R_E] and $T_{s,2}$ was used. This served to reduce heteroscedasticity and was preferred over a logistic function as a levelling off of R_E at higher $T_{s,2}$ was absent from this chronosequence. (ii) F_{NEP} was rejected for low u_* values at night and during daytime when downwelling photosynthetically active radiation (PAR) $<100\,\mu$mol m^{-2} s^{-1}. Only after reaching this threshold did the relationship between turbulence and flux disappear. (iii) Owing to ancillary sensor failure some gaps remained (<40 half-hours per annum on average), which were filled with the yearly median. In this paper, a positive value of F_{NEP} represents C uptake. All other C balance terms are always positive with the exception of P_N, which can be negative if $R_a > P_G$.

Continuous measurements of radiation, atmospheric, and soil state variables were made in parallel with the EC system. LAI (projected leaf area m^2 ground area m^{-2}) was interpolated between measurements made periodically, using either the LAI-2000 (LI-COR, Lincoln, NE, USA) or the point quadrat method, in the growing season at HDF88 and HDF00 and once yearly at DF49. Additional details regarding the EC system, ancillary measurements, LAI interpolation, and data processing protocols were given in Humphreys *et al.* (2006).

Half-hourly net primary productivity and component respiration calculations

Half-hourly fluxes of P_N, R_a, and R_h were calculated with a three-parameter, five-equation model based on mass balance of C ($F_{NEP} = P_G - R_E = P_N - R_h$ and $R_E = R_a + R_h$) using the following seven steps:

1. P_N was expressed as a function of two ratios (Griffis *et al.*, 2004)

$$P_N = P_G - R_a = P_G\left(1 - \frac{R_a/R_E}{1 + F_{NEP}/R_E}\right) = P_G\left(1 - \frac{\beta}{1+\theta}\right), \quad (1)$$

where β is the ratio of R_a to R_E and θ the ratio of F_{NEP} to R_E.

2. Equation (1) was then rearranged with β as a function of CUE, the ratio of P_N to P_G:

$$\beta = \left(1 - \frac{P_N}{P_G}\right)(1+\theta). \quad (2)$$

3. At this point independent estimates of annual CUE for temperate forests were used to bracket the range of β. Following Griffis *et al.* (2004) a lower limit of 0.47 (Waring *et al.*, 1998) and an upper limit of 0.60 (Gifford, 1994) were used to calculate an upper and lower limit of β, respectively:

$$\begin{aligned} \beta_{upper} &= 0.53(1+\theta) \\ \beta_{lower} &= 0.40(1+\theta) \end{aligned}. \quad (3)$$

© 2007 The Authors

Table 1 Chronosequence site and EC system characteristics

Site characteristics	Near mature stand	Pole/sapling stand	Clear cut
Site ID	DF49	HDF88	HDF00
Location	49°52.137′N, 125°20.120′W	49°31.180′N, 124°54.105′W	49°52.330′N, 125°17.537′W
Year stand established	1949	1988	2000
Stand age in 2005 (years)	56	17	5
Stand height in 2002 (m)	29.7	5.8	0.6
Stand density in 2002 (stem ha^{-1})	1150	1240	1500
Mean diameter in 2002 (cm)	28.3 (at breast height)	7.3 (at breast height)	1.02 (at base)
Range of maximum LAI ($m^2 m^{-2}$)	8.4 (assumed constant due to crown closure)	(6.6,7.2)	(0.8,2.5)
Site index (50 years)	35	29*	32
Stand history†	Clearcut, slash-burned, planted stock mixed with natural regeneration	Clearcut, broadcast burned, planted	Clearcut, planted
Stand size (ha)	130	110	32
Tree cover type	80% *Pseudotsuga menziesii*, 17% *Thuja plicata*, 3% *Tsuga heterophylla*	75% *Pseudotsuga menziesii*, 21% *Thuja plicata*, 4% *Abies grandis*	97% *Pseudotsuga menziesii*, 3% *Thuja plicata*
Understory description	Vanilla leaf deerfoot, oregon grape, mosses	Salal, oregon grape, fireweed, and bracken fern, Huckleberry	Grasses, ferns, herbs, woody shrubs: twinflower, honeysuckle rubrus spp., oregon grape
Mean annual temperature (°C)‡	8.4 (0.47)	9.7 (0.39)	8.9 (0.64)
Mean annual precipitation (mm)‡	1293 (288)	1471 (254)	1241 (104)
Soil classification	Humo-ferric podzol	Humo-ferric podzol	Humo-ferric podzol
Soil texture (top 40 cm)	Gravelly loamy sand	Loam	Gravelly loamy sand to sand
Elevation (m)	300	200	180
Flux tower height (m)	42	12	2.5
u_* threshold ($m s^{-1}$)	0.3	0.18	0.08
Three-axis sonic anemometer–thermometer (SAT)	Models 1012R2A (before April 2001) & 1012R3A (starting April 2001), Gill Instruments, Lymington, UK	Before January 2002: model CSAT3, Campbell Scientific Inc., Logan, UT, USA Starting January 2002: model R3, Gill Instruments, Lymington, UK	Model R3, Gill Instruments, Lymington, UK
CO_2/H_2O infrared gas Analyser (IRGA)	Closed-path LI-6262 IRGA, LI-COR Inc., Lincoln, NE, USA	Before January 2002: open-path LI-7500 IRGA, LI-COR Inc., Lincoln, NE, USA Starting January 2002: closed-path LI-6262 IRGA, LI-COR Inc., Lincoln, NE, USA	Closed-path LI-6262 IRGA, LI-COR Inc., Lincoln, NE, USA
Data coverage (% of all potential data measured)	96.6	88.3	89.2
Data rejected (% night-time data rejected due to low turbulence)	70.1	70.6	60.2
Measurement period	January 1998–December 2005	January 2002–December 2005	January 2001–December 2005

*Humphreys (2004), using 2002 age–height relationships, determined that HDF88 has a growth trajectory more similar to DF49. It is likely that the site index value for HDF88 is underestimated.

†DF49 and HDF88 are dominated by an even-aged overstory with only non-tree vegetation in the understorey. HDF00 has only 1 age class of trees present, those planted during the year of stand establishment. All stands are unthinned.

‡1 SD in parenthesis.

© 2007 The Authors

Table 2 Characteristics of MC simulation technique

	Range*			θ in 2004†		
Subpopulation	θ	CUE	Comments	DF49	HDF88	HDF00
I (night-time‡)	−1	*n/a*	• $P_N = -R_a$ • $-R_a$ calculated using β linearly interpolated between last valid (i.e. $\theta > -1$), data point before sunset to first valid point after sunrise • Only subpopulation without stochastic element	8817 (50)	8796 (50)	8814 (50)
II	[−1, −0.75)	[−∞, 0.53)	• $\beta \sim U$ (0.1, 0.13) • CUE $\propto \theta$ • Lower limit on apparent CUE approaches−∞	345 (2)	536 (3)	1723 (10)
III	[−0.75, 0.7)	0.53	• $\beta = f(\theta)$ • Only subpopulation where apparent CUE simplifies to $U \sim$ (0.47,0.60)	3442 (20)	4223 (24)	6138 (35)
IV	[0.7,∞)	(0.53, 1]	• $\beta \sim U$(0.68, 0.9) • CUE $\propto \theta$ • Upper limit on apparent CUE asymptotically approaches unity	4964 (28)	4013 (23)	893 (5)

Parameters used were CUE end points (0.47, 0.60) and $\Omega = 0.1$. Ranges of θ, apparent CUE, and β were calculated by applying the $\Omega = 0.1$ constraint and conserving mass balance of carbon (C). An example using subpopulation IV follows: Using Eqn (3) it is clear that $\beta_{upper} > 1$ when $\theta > 0.88$. This violates conservation of C (i.e. $R_a > R_E$ is impossible). Assuming that the smallest component respiratory flux is $\geq 10\%$ (i.e. $\Omega = 0.1$), this threshold becomes $\theta \geq 0.7$ with $\beta_{lower} = 0.68$, from Eqn (3), and $\beta_{upper} = 1 - \Omega = 0.9$. These end points are used in Eqn (4) to generate β^* when $\theta \geq 0.7$. Using the mean of $\beta \sim U$ (0.68, 0.9) = 0.79 to calculate the bracketed quantity in Eqn (4) with $\theta = 0.7$ gives mean apparent CUE = 0.53. This quantity monotonically increases and asymptotically approaches unity as $\theta \to \infty$. The remaining subpopulations were similarly derived.
*Lower and upper bounds for θ and mean apparent CUE by subpopulation.
†Number and percentage in parenthesis of all 17 568 half-hourly data values from 2004 in each subpopulation.
‡Night-time is all half-hours where block averaged downwelling photosynthetically active radiation was zero.
MC, Monte Carlo; CUE, carbon use efficiency.

4. These limits were adjusted on the assumption that R_E was always comprised both auto- and heterotrophic respiration with the smaller component, Ω, no $<10\%$ of the total ($\Omega = 0.1$): If β_{lower} was <0.1 or β_{upper} exceeded 0.9 the end points were recalculated (i.e. the end points based on the closest θ value where the relevant threshold was not exceed were used). This adjustment was needed when $\theta \leq -0.75$ or $\theta > 0.7$ (Table 2).
5. A random draw bounded by the upper and lower limit of β was then used in Eqn (1) as follows:

$$P_N = P_G\left(1 - \frac{\beta^*}{1+\theta}\right), \tag{4}$$

where β^* is the random draw and the bracketed quantity is apparent CUE, a half-hourly realization of CUE (discussed below). The retained value of half-hourly P_N was the mean of $n = 100$ bootstrap replicates (Efron & Tibshirani, 1998). Conceptually, the functional dependence of P_N on both CUE, through β [Eqns (2) and (3)], and θ, a measured ratio of two fluxes, temporally downscaled the annual CUE ratios to the half-hourly time scale.

6. The mean of $n = 100$ random draws of $\beta^*(= \overline{\beta})$ was used to calculate R_a and R_h

$$\begin{aligned} R_a &= \overline{\beta} R_E \\ R_h &= (1 - \overline{\beta}) R_E \end{aligned}. \tag{5}$$

7. At night-time when $P_G = 0$ and $\theta = -1$, Eqns (1)–(5) were unusable. Instead night-time β was linearly interpolated on a half-hourly basis between the last valid β before nightfall and the first valid β after sunrise. Night-time P_N (Table 2) was assumed equal to minus R_a (i.e. $P_N = -R_a$).

In sum, the model, Eqns (1)–(5), was constrained by F_{NEP}, P_G, and R_E (i.e. these fluxes were conditioned upon and treated as measurements irrespective of gap filling), mass balance of C, and three parameters: published lower and upper limits of CUE and Ω, the smallest

© 2007 The Authors

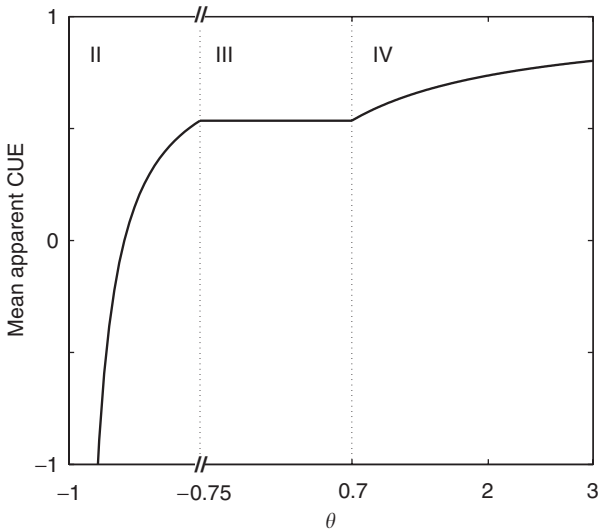

Fig. 1 Mean half-hourly apparent carbon use efficiency (CUE) as a function of θ (ratio of half-hourly F_{NEP} to R_E) partitioned into four subpopulations (roman numerals). Each subpopulation implements the Monte Carlo simulation technique for calculating P_N differently (Table 2). For subpopulation II mean half-hourly apparent CUE $\rightarrow -\infty$ as $\theta \rightarrow -1$. Values were cropped at -1 for clarity. Subpopulation I (night-time where $\theta = -1$) is not shown. Note the scale break at $\theta = -0.75$.

component respiratory flux. Given these constraints the half-hourly values of θ effectively partitioned the population of all half hours into four distinct subpopulations (Fig. 1, Table 2). It is noteworthy that apparent half-hourly CUE was neither constrained by the CUE end points used nor was it constant on subyearly time scales. While observations of CUE are typically on time scales of 1 year, EC-based estimates of P_G:R_E, at this chronosequence and elsewhere (Falge *et al.*, 2002), varied seasonally. Assuming a constant CUE with variable P_G:R_E requires $F_{NEP} + R_a = 0$ or, more importantly, $F_{NEP} < 0$ at all times. Furthermore, using only mass balance it can be shown that, for any half-hour where $R_a > P_G > 0$, P_N and CUE must be negative. As θ trends towards -1, indicating that most assimilates are being used in respiratory processes, CUE approaches $-\infty$. In this study, CUE typically varied between -10 and 1. Night-time CUE was assumed to be undefined and daytime CUE in the absence of P_G set to zero.

Finally, gap filling produced some negative values of P_G and R_E (e.g. modelled daytime $R_E < |$measured $F_{NEP}|$ and $F_{NEP} < 0$). This arose from applying mass balance to modelled values that required extrapolation beyond the range of data. Such values (<2% per annum on average) were retained for yearly totals but were assumed zero for daytime P_N. This caused departures from C balance closure. For R_E ($= R_h + R_a$) annual C closure was, averaged across all site years, within 1% or ca. $1\,g\,C\,m^{-2}$ and within 4% or ca. $10\,g\,C\,m^{-2}$ for P_N ($= P_G - R_a$).

Uncertainty estimates for C balance terms

Random error [i.e. the uncertainty used in constructing confidence intervals (CIs)] was estimated using MC simulation and error propagation. CIs exclude systematic errors (cf. Moncrieff *et al.*, 1996; Law *et al.*, 2002). However, previous work at DF49 (Morgenstern *et al.*, 2004) indicated that photoinhibition changes annual totals by <10% without altering year-to-year trends. Similarly, advection was addressed by excluding night-time data under low turbulence.

Standard errors (SE) were calculated as follows:

1. For each site year half-hourly F_{NEP} and R_E were generated 100 times using MC simulation. F_t, the true flux, was assumed within $\pm 20\%$ (Wesely & Hart, 1985) of each measured value: $F_t \sim U(0.8F_m, 1.2F_m)$, where F_m is the measured flux. The end points of the uniform distribution for modelled F_{NEP} and R_E values were $\pm 10\,\mu mol\,m^{-2}\,s^{-1}$ to reflect gap filled-induced errors (Morgenstern *et al.*, 2004). Half-hourly SE was the standard deviation (SD) across 100 realizations of F_t. Yearly SE was then calculated using error propagation of a sum (summation in quadrature: Lo, 2005) using the normalized autocorrelation at lag 1.
2. For daytime half-hourly P_N the SD across the 100 half-hourly bootstrap replicates, Eqn (4), was the SE for that datum. Night-time values were linearly interpolated between the last SD before nightfall and the first valid SD after sunrise. Yearly SE was the sum of all half-hourly SEs. In contrast to F_{NEP} and R_E, this form of error propagation represents a worst-case scenario and was meant to penalize the distance between measured F_{NEP} and the MC-derived fluxes [i.e. Eqns (1)–(5)].
3. For P_G, R_a, and R_h SEs were calculated using mass balance (e.g. yearly P_G SE was the sum of the yearly SEs for F_{NEP} and R_E). As for P_N this was based on the worst-case scenario.

Data analysis

C balance terms were temporally aggregated (5 days or annual time step) and converted from CO_2 fluxes to mass C. Initially, 5-day ensemble means of the C balance, intermediate variables from Eqns (1)–(5), air temperature (T_{air}, °C), vapour pressure deficit (VPD, kPa) as a proxy for water stress (sensu Jolly *et al.*, 2005), radiation (PAR, $\mu mol\,m^{-2}\,s^{-1}$), and flux uncertainty were used to investigate seasonal trends. For CUE 5-day ensemble medians were used instead. CUE was always

© 2007 The Authors

negatively skewed (recall: CUE $\rightarrow -\infty$ as $\theta \rightarrow -1$) with a mean that was sensitive to large negative values. The use of median ensembles dampened this effect and served to highlight seasonal trends as opposed to short-term (<1 day) events. The investigation of seasonality was intended as a heuristic to enable a better understanding of the MC simulation technique. Subsequent analyses focussed on annual totals and stand age as an explanatory variable. The following cardinal points of the stand age–C balance response surface were of interest: the carbon compensation point, maximum annual fluxes, and total fluxes assuming a rotation age of 56 years. Four efficiencies (i.e. the ratio of two C balance terms) were calculated either based on annual or chronosequence fluxes: R_h:R_E, P_N:P_G, F_{NEP}:P_G, and F_{NEP}:R_E. These efficiencies were used to quantify chronosequence status in terms of soil C mining (R_h:P_N), the efficiency of P_G in phytomass production (P_N:P_G), sink–source status (F_{NEP}:P_G), and the efficiency of C uptake (F_{NEP}:R_E, i.e. θ on an annual basis).

Annual MC-simulated P_N values were then compared with growth and yield data. Coble *et al.* (2001) studied both total above- and belowground P_N in western Montana, USA, at sites that included Douglas-fir dominated stands with comparable site indices with those on Vancouver Island. Belowground P_N was 75–90% of aboveground P_N or, more generally (cf. Coble *et al.*, 2001, Fig. 5): $P_{N,B} = 0.6663P_{N,A} + 431.63$, where the second subscripts A and B denote above- and belowground. This relationship was used to scale up growth and yield data from TIPSY version 3.2 (Table Interpolation Program for Stand Yields; Mitchell *et al.*, 2000). TIPSY is a growth and yield model applicable to this chronosequence where stands are indexed by region and site index. TIPSY output was converted to g C using an average wood density of 510 kg DM m^{-3} (Simpson & TenWolde, 1999) and then scaled from aboveground tree bole P_N to total P_N with the relationship presented in Coble *et al.* (2001).

The behaviour of Eqns (1)–(5) using the base parameterization was investigated using running 5-day means of apparent CUE, θ, and β. Also, static (either β or CUE constant) and dynamic (CUE and β were treated as random variables) reparameterizations (i.e. sensitivity analyses) were used to recalculate the 17-year data record in terms of annual totals and 5-day means. Initially, a fixed CUE (= 0.5) was assumed to contrast the technique as described. As mass balance of C was not conserved on the half-hourly time scale, only annual C balance estimates were recalculated as follows: $P_N = 0.5P_G$, $R_a = 0.5P_G$, and $R_h = R_E - 0.5P_G$. Another static recalculation was performed assuming a fixed β (= 0.5). Gap-filled data were postprocessed independently of Eqns (1)–(5) using: $0.5R_E = R_a = R_h$ and $P_N = P_G - 0.5R_E$. The second, dynamic, component of the sensitivity analysis involved changing the CUE end points and Ω by 0.05 in both directions. We recalculated P_N, R_a, and R_h on the half-hourly time scale using (i) $\Omega = 0.05$ and 0.15 with the CUE end points constant at (0.47, 0.60), and (ii) using all possible combinations of the base CUE end points ± 0.05 and $\Omega = 0.1$. All analyses were performed using MATLAB (version 6.5.1 R13, The Mathworks Inc. Natick, MA, USA).

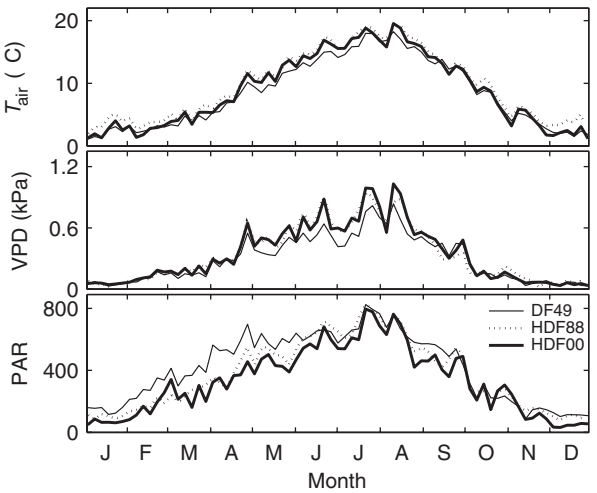

Fig. 2 Five-day ensemble means of air temperature at eddy height (T_{air}, °C, top panel), vapour pressure deficit at eddy height (VPD, kPa, middle panel), and daytime average photosynthetically active radiation (PAR, μmol m^{-2} s^{-1}, bottom panel): HDF00 (2001–2005, thick line), HDF88 (2002–2005, dotted line), and DF49 (1998–2005, thin line).

Results

Seasonality of the C balance

The 5-day ensemble means of PAR, T_{air}, and VPD were similar at all sites (Fig. 2) and were important controlling factors for the seasonal course of the C balance. At all sites (Figs 3–5) F_{NEP} peaked before all three meteorological variables suggesting that the temperature response of P_G (linear) was outperformed by that of R_E (exponential; Schwalm *et al.*, 2005). At DF49, higher presummer levels of PAR corresponded to the highest rate of C sequestration and all C terms except for F_{NEP} were largely in phase throughout the ensemble year, peaking in late July (Fig. 5). The decoupling of peak C balance terms was intermediate at HDF00 and most extreme at HDF88 (Figs 3 and 4). An additional commonalty for the chronosequence was that $R_h > R_a$ except for the early part of the ensemble year at DF49 when F_{NEP} was highest.

© 2007 The Authors

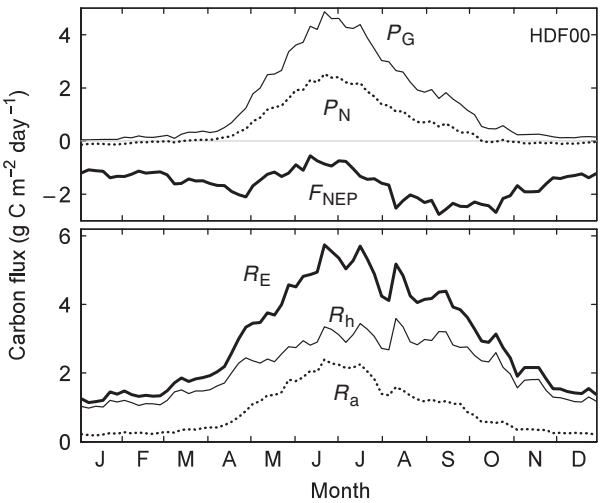

Fig. 3 Five-day ensemble means of all six carbon fluxes at HDF00 for 2001–2005. Top panel shows P_G (thin line), P_N (dotted line), and F_{NEP} (thick line). Bottom panel shows R_h (thin line), R_a (dotted line), and R_E (thick line).

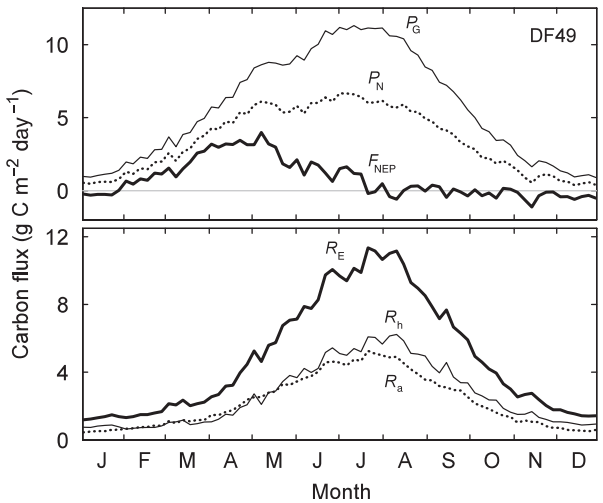

Fig. 5 Five-day ensemble means of all six carbon fluxes at DF49 for 1998–2005. Top panel shows P_G (thin line), P_N (dotted line), and F_{NEP} (thick line). Bottom panel shows R_h (thin line), R_a (dotted line), and R_E (thick line).

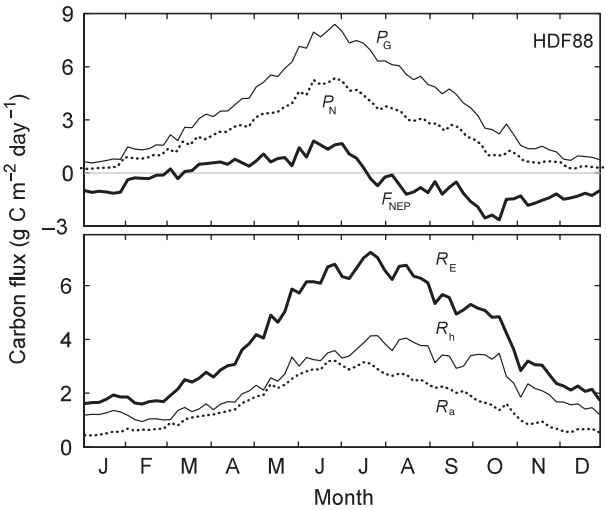

Fig. 4 Five-day ensemble means of all six carbon fluxes at HDF88 for 2002–2005. Top panel shows P_G (thin line), P_N (dotted line), and F_{NEP} (thick line). Bottom panel shows R_h (thin line), R_a (dotted line), and R_E (thick line).

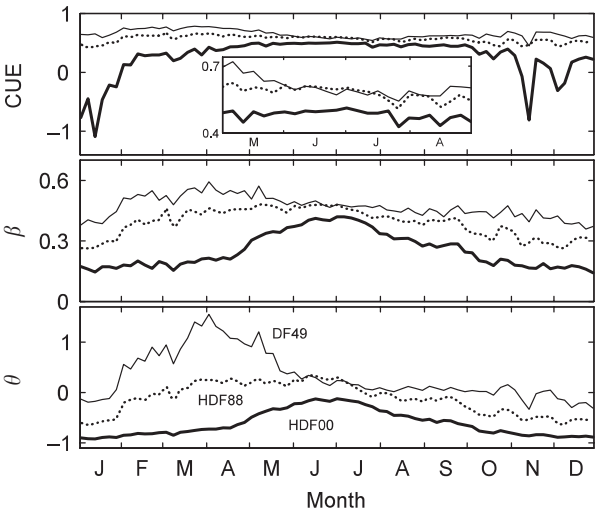

Fig. 6 Five-day ensemble means of carbon use efficiency (CUE; median based, top panel), β (ratio of half-hourly R_a to R_E) used in calculating component respiratory fluxes (middle panel), and θ (ratio of half-hourly F_{NEP} to R_E, bottom panel): HDF00 (2001–2005, thick line), HDF88 (2002–2005, dotted line), and DF49 (1998–2005, thin line). Inset in top panel highlights CUE dynamics from May through August.

CUE from May through July ranged from 0.4 to 0.7 with HDF00 exhibiting the most variability. At DF49 Both β and θ peaked before F_{NEP} (Fig. 6) in March. This corresponded to low VPD (<0.3 kPa) and cooler temperatures (<5 °C; Fig. 2). At this point of the year there was less biological activity and a smaller proportion of R_E relative to F_{NEP}. CUE peaked with F_{NEP} and was generally higher in cooler, less water-limited periods of the year (low VPD).

At the younger sites, peak CUE, β, and θ were in phase with peak F_{NEP}. This peak occurred before (but closer to than for DF49) the onset of high summer temperatures and increased water stress (Fig. 6). The different seasonal cycles between the two young stands and the mature site relate to the importance of C cycling in nontree vegetation. At HDF00 and HDF88, ca. 80% and 50% of the total LAI was nontree. In contrast to the dominant Douglas-fir, the nontree vegetation did have a

© 2007 The Authors

distinct growing season. This shifted peak F_{NEP} relative to DF49 as each nontree species had a different P_G and R_E response through time. DF49, with ca. 95% of total LAI in Douglas-fir, reflected the physiology of the overstory. It is noteworthy that seasonal 5-day SEs were proportional to flux magnitude for the entire C balance. However, the magnitude of this uncertainty was never large enough to remove a seasonal trend described for either P_N (Fig. 7) or any other flux (not shown).

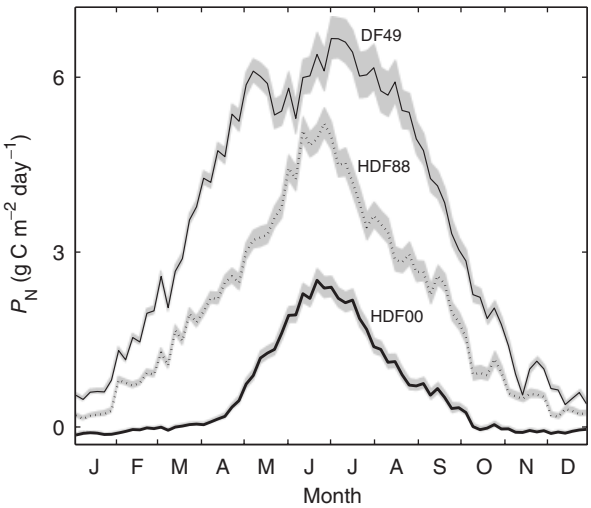

Fig. 7 Five-day ensemble means of P_N with confidence interval for all sites: HDF00 (2001–2005, thick line), HDF88 (2002–2005, dotted line), and DF49 (1998–2005, thin line). The vertical extent of the grey area at any point in time shows a 95% confidence interval of the ensemble mean flux.

Linkages between intermediate variables and C fluxes manifested themselves as follows: (i) β and θ were in phase and proportional throughout the year. For DF49 in particular, the relationship between θ and β weakened as θ increased (Fig. 6) but persisted. As $\theta \to -1$, $P_G \to 0$; this removed synthesis respiration from R_a and caused β to decrease. (ii) θ and CUE were proportional, suggesting the proportion of R_a per unit P_G decreases with increasing R_a (Shirke, 2001; Vose & Ryan, 2002). Overall, the seasonality of weather and the distribution of θ, when aggregated annually, produced yearly flux totals of P_N, R_a, and R_h as scale-emergent properties of the chronosequence. For example, annual CUE is determined by the distribution of θ over the course of the year. A sink (DF49) has more θ values in subpopulation IV, causing annual CUE to increase. A source (HDF00) will have fewer θ values in subpopulation IV, which acts to decrease annual CUE. It is also noteworthy that neither half-hourly β nor half-hourly CUE are constrained by the end points used in model formulation.

C balance as a function of stand age

Annual C fluxes (Table 3) by and large increased with increasing stand age (Fig. 8). R_h was more conservative compared with the other trajectories with the relatively

Table 3 Annual totals of all carbon balance terms with standard error in parenthesis

		Annual Fluxes (g C m^{-2} yr^{-1})					
Site	Year	P_G	F_{NEP}	R_E	P_N	R_h	R_a
HDF00	2001	166 (47)	−571 (21)	737 (27)	47 (11)	584 (31)	157 (58)
	2002	408 (44)	−606 (18)	1013 (26)	150 (21)	738 (39)	278 (65)
	2003	519 (43)	−614 (17)	1135 (25)	199 (25)	809 (47)	332 (68)
	2004	661 (43)	−642 (18)	1303 (26)	267 (31)	902 (48)	405 (74)
	2005	849 (45)	−450 (19)	1295 (26)	392 (35)	857 (55)	453 (81)
HDF88	2002	1178 (48)	−168 (20)	1348 (27)	665 (40)	824 (61)	526 (88)
	2003	1164 (48)	−147 (21)	1313 (27)	630 (41)	778 (63)	536 (89)
	2004	1407 (47)	−199 (21)	1606 (27)	768 (49)	963 (69)	644 (96)
	2005	1610 (46)	−39 (21)	1652 (27)	931 (51)	963 (71)	687 (97)
DF49	1998	2059 (46)	296 (20)	1766 (26)	1253 (63)	959 (82)	813 (109)
	1999	1985 (46)	328 (20)	1659 (26)	1230 (59)	900 (79)	760 (106)
	2000	2063 (46)	337 (20)	1725 (26)	1280 (59)	931 (79)	794 (105)
	2001	2045 (46)	376 (20)	1671 (26)	1273 (60)	891 (80)	779 (106)
	2002	1926 (46)	219 (20)	1708 (26)	1150 (60)	917 (80)	790 (106)
	2003	2011 (46)	318 (20)	1695 (26)	1230 (60)	900 (80)	795 (106)
	2004	2272 (46)	194 (22)	2078 (20)	1326 (74)	1125 (94)	954 (120)
	2005	2245 (47)	277 (22)	1972 (20)	1353 (69)	1070 (89)	903 (115)
Total*		91 700	2100	89 600	53 100	51 000	38 600

*Flux totals (g C m^{-2} rotation^{-1}) assuming a 56-year rotation and quadratic flux–stand age relationships (Fig. 8).

© 2007 The Authors

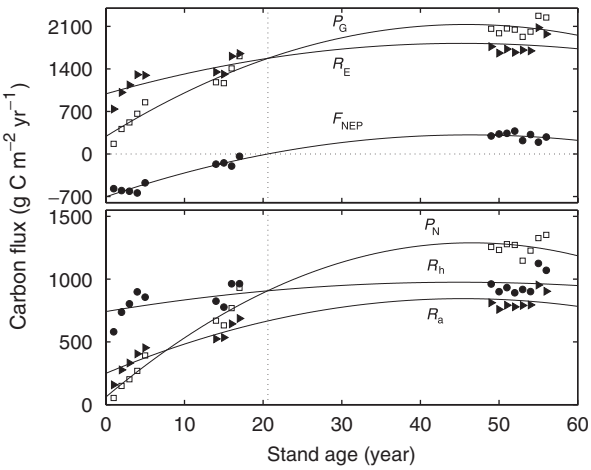

Fig. 8 Annual carbon balance fluxes as a quadratic function of stand age. Top panel shows P_G (□), R_E (▲), and F_{NEP} (•) for all 17 site years. Bottom panel shows P_N (□), R_a (▲), and R_h (•) for all complete site years. Horizontal dashed line is zero reference line. Vertical dashed lines demarcate the intersection of modelled P_G with R_E, P_N with R_h, and F_{NEP} with the zero reference line. All three expressions of the canopy compensation point occur at stand age 20 years.

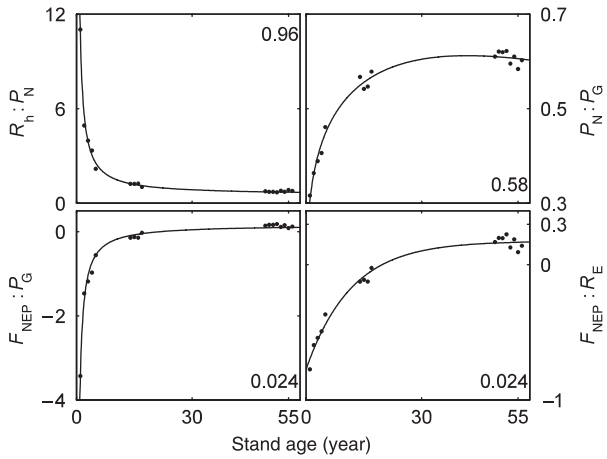

Fig. 9 Four carbon (C) balance efficiencies, from upper-left panel then clockwise: R_h:P_N, P_N:P_G, F_{NEP}:R_E, and F_{NEP}:P_G (all in g g^{-1}) as a function of stand age. Fitted lines (same order): hyperbolic fit: $y = a + b/x$, Hoerl: $y = ab^x x^c$, hyperbolic, and modified exponential: $y = a(b - \exp[-cx])$. Values inset in each panel are chronosequence efficiencies calculated by using quadratic C balance–stand age relationships (Fig. 8) from stand ages 1 through 56 years.

large values at initiation stand suggesting that a residue-based flush of respiration occurred shortly after harvest. Uncertainty within years generally increased as follows: $F_{NEP} < R_E < P_G < P_N < R_h < R_a$. (Table 3), mirroring the increase in the proportion of modelled values. Between years the MC-simulated quantities typically showed higher (and more variable) SEs whereas F_{NEP}, R_E, and P_G were more conservative.

All four efficiencies changed over time with the largest change occurring between HDF00 and HDF88 (Fig. 9). Until stand age ca. 24 years, R_h:P_N was greater than unity. F_{NEP}:P_G switched from negative to positive at ca. 20 years. This was the same as the canopy compensation point calculated using annual flux–stand age relationships (Fig. 8). CUE for the entire chronosequence was 0.58. The chronosequence was a weak sink as evinced by chronosequence F_{NEP}:P_G (= 0.024), F_{NEP}:R_E (= 0.024), and a total F_{NEP} of ca. 2100 g C m^{-2}. This represented a small fraction of total P_G (= ca. 91 700 g C m^{-2}) and R_E (= ca. 89 600 g C m^{-2}) across the 56-year rotation (Table 3, bottom row).

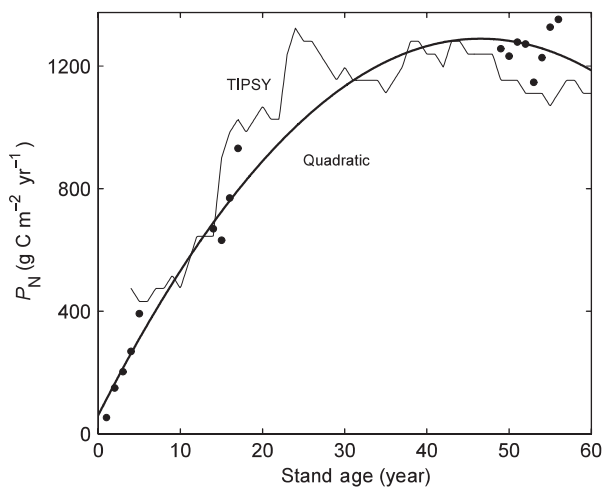

Fig. 10 P_N for all 17 complete site years (•) as estimated via Monte Carlo simulation, Table Interpolation Program for Stand Yields (TIPSY) output (thin line), and $P_N \sim$ stand age quadratic model (thick line). Gross volume from TIPSY was scaled from m^3 ha^{-1} yr^{-1} to g C m^2 yr^{-1} via wood density, a relationship between aboveground and total P_N given in Coble *et al.* (2001), and assuming 1 g C = 2 g DM. Model output began at stand age 5 years due to the breast height requirement of TIPSY.

Comparison of annual P_N totals to stand table output

Scaled TIPSY output over stand age was in good agreement with MC-simulated P_N (Fig. 10). As TIPSY output referenced only the tree bole portion above breast height (1.3 m) of P_N, divergences in the two trajectories were expected. TIPSY did not show aboveground P_N until tree height reached this threshold, whereas a baseline belowground P_N appeared due to the scaling relationship used. This made comparisons at HDF00 speculative as all trees were <1.3 m tall and the majority of vegetation nontree. P_N for HDF88 was overesti-

© 2007 The Authors

Table 4 Summary of sensitivity analysis for the three MC stimulated fluxes in 2004

		Dynamic		$\beta = 0.5$		CUE = 0.5	
Site	Flux	Raw change*	Fractional SE†	Raw change	Fractional SE	Raw change	Fractional SE
DF49	P_N	(−46, 44)	0.7	−93	1.3	−190	2.6
	R_a	(−44, 46)	0.4	86	0.7	183	1.5
	R_h	(−46, 44)	0.5	−86	0.9	−183	2.0
HDF88	P_N	(−29, 28)	0.6	−165	3.4	−66	1.3
	R_a	(−28, 29)	0.3	160	1.7	60	0.6
	R_h	(−29, 28)	0.4	−160	2.3	−60	0.9
HDF00	P_N	(−27, 23)	0.9	−259	8.4	62	2.0
	R_a	(−23, 27)	0.4	247	3.3	−74	1.0
	R_h	(−27, 23)	0.6	−247	5.1	74	1.5

*Raw change is the distance ($g\,C\,m^{-2}\,yr^{-1}$) between the annual total under the base parameterization and the recalculation. For dynamic runs the range (min, max) is given.
†Fractional SE is the ratio of the absolute value of the raw change over the SE. For dynamic recalculations the highest value is given; mean values are all ca. 0.1.
MC, Monte Carlo; CUE, carbon use efficiency.

mated and underestimated for DF49. This was likely an artefact of TIPSY, which uses site index, the expected height of dominant trees at stand age 50 years, to adjust growth trajectories. The mean site index used (= 32 m) for the scaling exercise was larger than for HDF88 and smaller for DF49. In general, the two estimates became closer for stand age >30 years.

Sensitivity analysis of MC technique

As changes in annual totals and 5-day ensemble means of P_N, R_a, and R_h were similar in terms of ranking and magnitudes at each site for all years only 2004 annual totals and 5-day ensemble means from DF49 are presented. Apparent CUE and β at longer than half-hourly time scales is determined by the daytime distribution of θ. Changes in Ω altered the width of subpopulation III relative to θ. The range under the original parameterization was (−0.75, 0.70) but changed to (−0.88, 0.80) at $\Omega = 0.5$ and (−0.63, 0.79) at $\Omega = 0.15$. As the width of subpopulation III changed, the amount of half-hourly data points along the nonlinear portion of the CUE response surface also changed (Fig. 1). Changing CUE end points had a similar effect to altering Ω. The range of θ in subpopulation III widened as the distance between the CUE end points decreased and vice versa. For all dynamic parameter combinations annual totals were closest (<1 SE and $< \pm 50\,g\,C\,m^{-2}\,yr^{-1}$) to the standard parameterization (Table 4). Static parameterizations diverged to a greater extent (0.6 ≥ SE8.4 and ±60 to $260\,g\,C\,m^{-2}\,yr^{-1}$). Dynamic 5-day ensemble means were clustered around the base parameterization

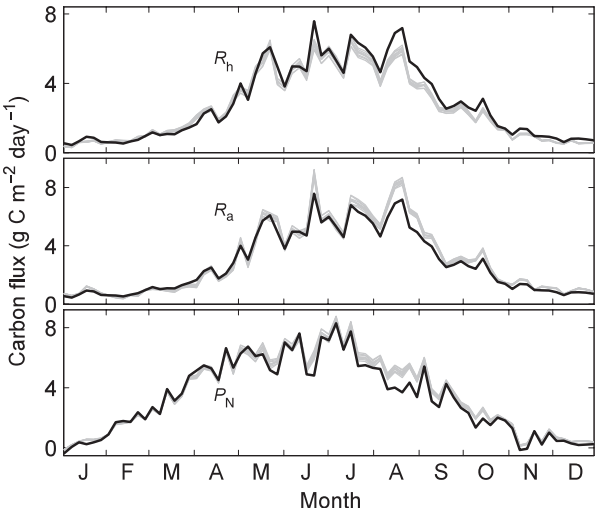

Fig. 11 Five-day ensemble means of recalculated (from top to bottom) R_a, R_h, and P_N for DF49 in 2004: dynamic recalculations [grey lines, carbon use efficiency (CUE) and β treated as random variables, base parameterization included] and static recalculation (thick line, $\beta = 0.5$).

($\pm 0.2\,g\,C\,m^{-2}\,5\,day^{-1}$). The static runs, however, had a mean discrepancy of ca. $1.5\,g\,C\,m^{-2}\,5\,day^{-1}$ in August through September for all MC-simulated fluxes (Fig. 11). Overall, the magnitude of run-to-run changes was driven by differing end points in the range of θ, β, and CUE relative to the four subpopulations under the base parameterization. For static runs the effect was larger due to holding β or CUE fixed.

© 2007 The Authors

Discussion

Ecological insights from modelled C balance trajectories

Given that the C balance–stand age response surface is relatively sparse; conditioning on the interpolated relationships allows an examination of how these fluxes change through time. The model used to interpolate across missing stand ages predicted three instances of when the chronosequence switches from a source to a sink of C (i.e. the canopy compensation point): $F_{NEP} = 0$, $P_N = R_h$, and $P_G = R_E$, at stand age 20 (Fig. 8). The modelled trajectories, despite this congruence, did not completely capture the site-specific interannual dynamics of the C balance, particularly at HDF00. The distribution of HDF00 values in annual flux–stand age space suggested that, initially, the chronosequence should be expected to 'bottom out' before negative F_{NEP} would increase. Three points confound this expectation: (i) 2004 was the warmest year for HDF00, HDF88, and the second warmest for DF49. Higher mean annual temperatures (MAT) enhanced R_E more so than P_G resulting in the lowest F_{NEP} values for all three sites. (ii) IAV at HDF00 (Fig. 8) is larger than the other two sites due to the change in functional parameters attendant with a 1-year increase in stand age for a 5-year-old stand. This suggested that viewing the 5-year record at HDF00 as pseudo-replicates as a means to quantify IAV is suspect and that a stand age effect was possibly confounded with an IAV effect. (iii) The incorporation of residue and higher soil temperatures in the recently clearcut HDF00 (Humphreys *et al.*, 2005) could have potentially facilitated an initial burst of R_h and corresponding decrease in F_{NEP}. However, it is speculative to disambiguate the effects of higher MAT, IAV, stand age–growth relationships, and a burst in R_h. The regularity and duration of a postharvest increase in R_E or a burst in R_h has also not been established (cf. Kowalski *et al.*, 2004).

Despite the scatter of R_h and R_E, relative to P_N both exhibited well-defined trends (Fig. 9). Shortly after the canopy compensation point R_h:P_N was less than unity, suggesting that the chronosequence began accumulating soil C after switching to a sink. This assumes a simple model, whereby accumulated P_N reverts to the soil C pool via mortality. As the chronosequence value was ca. 1, the effect of the management regime in this stand (harvest) would negate any soil C inputs over the life of the stand.

The longer-term, successional changes from stand to stand were better captured by the modelled trajectories as evinced by an intercomparison with other chronosequences: The consensus of EC chronosequence studies of F_{NEP}, including this study, is that F_{NEP} initially increases with age and all chronosequences serve as sinks of C when F_{NEP} is largest. This has been shown for a fire-dependent successional gradient (ca. 400 years fire cycle) in central Siberia, Russia (Röser *et al.*, 2002), *Pinus sylvestris* in southern Finland (Kolari *et al.*, 2004), *Pinus ponderosa* in semiarid central Oregon, USA (Law *et al.*, 2003), *P. menziesii* in Wind River Valley, Oregon, USA (Chen *et al.*, 2002), as well as *P. banksiana* (Howard *et al.*, 2004) and *Picea mariana* (Bond-Lamberty *et al.*, 2004c), both in the southern Canadian boreal forest. Similarly, the initial increasing trend of chronosequence P_N as a function of stand age mimicked growth trajectories seen in growth and yield tables (Figs 8 and 10) and recent studies of forest metabolism (e.g. Mund *et al.*, 2002; Law *et al.*, 2003, Bond-Lamberty *et al.*, 2004c; Howard *et al.*, 2004; Pregitzer & Euskirchen, 2004).

In their metastudy of EC-based and biometrical studies, Pregitzer & Euskirchen (2004) presented evidence that the P_N and F_{NEP} of temperate forests were highest at intermediate stand ages (11–30 years). The modelled trajectories here continued to increase through this age band. Reasons for this discrepancy were likely related to the variability in the metastudy results, and the lack of data between HDF88 and DF49. Pregitzer & Euskirchen (2004) reported large CV values by age class (>60%, with a maximum of >1000%) with overlap between classes evident. Temperate rainforests were also not well represented. Nonetheless, it is plausible that the maximal annual rates of C sequestration and biomass accumulation have not been observed and that this corresponds to a stand age between HDF88 and 30 years.

The initial rise in P_G with stand age (Fig. 8) is well established (Ryan *et al.*, 2004). For R_E–stand age relationships less information was available. Not all EC-based studies include the calculation of R_E. In general, and in this chronosequence, R_E increased with stand age only to decrease, with varying degrees of steepness, after various age thresholds (e.g. Anthoni *et al.*, 2002; Röser *et al.*, 2002; Kolari *et al.*, 2004). Information on R_a–stand age relationships is absent from the literature. There are only studies that deal with LAI and/or stand age and a component of R_a (e.g. foliage respiration: Anthoni *et al.* [2002]). For studies focussing on R_h, R_s is frequently used instead. This confounded efforts to compare and contrast the MC-derived R_h here with other published reports. Griffiths & Swanson (2001) found an increase in R_s over time in a harvested *P. menziesii* chronosequence at H. J. Andrews Experimental Forest, Oregon, USA. Studying an afforestation chronosequence of *Picea abies* in Italy, Thuille *et al.* (2000) showed an initial burst in R_s followed by a decreasing trend until stand age 30 years after which an increase set in. But in both cases R_s was not measured for a full

© 2007 The Authors

calendar year. Bond-Lamberty *et al*. (2004b) found a pattern similar to P_N but with considerable noise. Pregitzer & Euskirchen (2004) suggested that R_h was highest in younger stands and declined with increasing stand age. Law *et al*. (2003) found no relationship between stand age and R_h in *P. ponderosa* stands in semiarid central Oregon, USA. A similar lack of relationship was observed in this chronosequence.

In addition to the broad qualitative agreement with other chronosequences, the MC-derived fluxes have the advantage of being based on direct linkages between measured quantities (i.e. F_{NEP}, R_E, and P_G). This is in contrast to applying an invariant point estimate (e.g. CUE = 0.5, Waring *et al*., 1998) of CUE to arrive at an annual value. Indeed, using the CUE midpoint (= 0.535) overestimated CUE for HDF00 and underestimated CUE for the two older sites. Furthermore, there is a large body of evidence contradicting convergence in CUE (e.g. Gifford, 2003). Using a point estimate of CUE annually also does not allow for the resolution of R_a and R_h via linkages to θ and β. Estimated annual CUE was not, despite considerable overlap, constrained by the CUE limits used to generate end points for β (i.e. the parameter values for the limits of CUE do not, *a priori*, determine actual CUE). As the initial end points of CUE represent a range of long-term values, actual annual CUE becomes a scale emergent property of Eqns (1)–(5).

Insensitivity of recalculations

Ideally, the MC technique as described should be relatively insensitive to the initial values for the CUE end points and Ω. Insensitivity is desirable as the exact values of the CUE end points are unknown but logically constrained between zero and unity. For this study the end points chosen roughly correspond to the interquartile range (IQR) of published values for temperate forested biomes. Similarly, while assuming that both respiratory fluxes co-occur is plausible (cf. Janssens *et al*., 2001) the exact value of Ω is unknown. Any annual total from a given dynamic reparameterization was <1 SE or $50\,\mathrm{g\,C\,m^2\,yr^{-1}}$ from the base parameterization (i.e. less than one half-width of a 95% CI). This suggested that, statistically, any reparameterization will arrive at the same answer and that the desired insensitivity, relative to the parameter perturbations, is present.

In contrast, the two static reparameterizations resulted in annual totals that were more different than the base parameterization results. However, both static recalculations, while serving as useful tools to bracket uncertainty, can be discounted. An invariant half-hourly CUE has not been experimentally validated. Any half-hour where $R_a > P_G$ yields a negative CUE. Also, annual CUE values reported for forested ecosystems do not converge on a constant. Similarly, the diurnal and seasonal cycle of P_G leads to different values of CUE for the same value of P_G as a function of R_a and its sensitivity to temperature (cf. Goetz & Prince, 1999). Finally, the assumption of CUE = 0.5 does not allow for the calculation of P_N, R_h, and R_a on the half-hourly time scale as mass balance of C is not conserved; β is pushed over unity and the fixed proportionality constant makes any adjustment via Eqns (1)–(5) impossible. Synthesis work on chamber-measured R_s and biometrical R_a provides some indication that an invariant β is inappropriate. Bond-Lamberty (2004a, b) showed that RC, the ratio of R_a to R_s, varies with stand age, magnitude of R_s, seasonality, and temperature. Strictly speaking, RC is not equivalent to β. But the existence of a compensatory aboveground R_a flux to force a constant β is unlikely. Similarly, Ryan *et al*. (1997) showed clear seasonality in R_a and components thereof. Such seasonal trends in β are visible in this chronosequence.

While the insensitivity of the technique, as well as the broad agreement with TIPSY and other chronosequences are encouraging such intercomparisons are not validation in the strictest sense. However, there are currently no known techniques, apart from the MC method detailed here, to directly estimate half-hourly P_N. Similarly, while techniques exist to calculate component respiratory fluxes using RC, these are not associated with tower-sized footprints. Scaling is an issue as there is no *a priori* reason to assume that the source strength of the chamber footprint is identical to that of the tower footprint, particularly if chamber placement is subjective and/or insufficient to address spatial variation within the tower footprint. Finally, as isotope data become more widespread validation of the component respiratory fluxes, and, by mass balance, P_N, will be possible at the half-hourly time scale as opposed to the annual fluxes discussed here.

Conclusions

An additional postprocessing step of EC data was developed which extends the usual gap filling procedure to allow for estimates of three additional half-hourly fluxes: P_N, R_a, and R_h. Conceptually, annual biome-specific estimates of CUE were localized (from biome to site) and down-scaled (from year to half-hour) using a three-parameter five-equation model of how CO_2 is partitioned across a six-term C balance. This was achieved through an explicit linkage to θ, a measured quantity. The strengths of this approach are its relative parameter insensitivity, parsimony, ability to resolve seasonal trends, and qualitative agreement with other

© 2007 The Authors

estimates of these three fluxes. The latter was evinced by stand table derived estimates of annual P_N and chronosequence behaviour that corresponded to trends observed at other sites. Weaknesses of this method are the large data burden required for quantitative validation and the dependence on F_{NEP}. The trajectories for P_N, R_a, and R_h have no equivalent in published EC reports. While future validation of this additional post-processing step is important, particularly at subyearly time scales, the utility of estimating F_{NEP}, R_E, P_G, as well as P_N, R_a, and R_h from EC data is immense.

The seasonal cycle of the C balance changed as a function of stand age. The time between peak rates of C sequestration, maximum CUE, and maximum β vs. summer weather (high T_{air} and high water stress) increased with stand age. In contrast, P_G and R_E always peaked with T_{air} highlighting their strong temperature dependency.

Over the life of the stand this chronosequence was a weak sink with a CUE of 0.58. CUE changed throughout the 56-year period and was lowest at HDF00 and highest as DF49. Current management practices will result in soil C mining in this chronosequence.

The modelled C trajectories for this chronosequence matched well with published reports from other forested biomes and growth and yield data. While interpolation was data based, as opposed to process based, this chronosequence suggests that all flux terms increase with age shortly after stand establishment. However, observations of maximum annual fluxes are not included in the extensive data set discussed here. These can only be inferred from the relationships presented and interpolation between the end points of the stand age continuum.

Augmenting the stand age response surface would greatly aid in quantifying cardinal points of the C budget through time. However, the infrastructure required to maintain a chronosequence of EC towers is immense and such efforts are not widespread. Ultimately, researchers will need to find a mechanism to sensibly interpolate between observed stand ages along a chronosequence, extrapolate to larger functional groups, and, ultimately, characterise the C balance of forest ecosystems through time. We believe that a model-based treatment of C balance terms coupled with the additional postprocessing steps for P_N, R_h, and R_a are useful tools to investigate C balance dynamics.

Acknowledgements

Funding for this research was provided by the Fluxnet Canada Research Network (FCRN), Canadian Foundation for Climate and Atmospheric Sciences (CFCAS), and BIOCAP Canada Foundation for CRS; and a Natural Science and Engineering Research Council of Canada (NSERC) Operating Grant for TAB. We also thank the numerous technicians, students, and research fellows that contributed to data collection and processing. Finally, the helpful comments of Dennis Baldocchi, Nina Buchmann, and six anonymous reviewers are acknowledged.

References

Amiro B (2001) Paired-tower measurements of C and energy fluxes following disturbances in the boreal forest. *Global Change Biology*, **7**, 253–268.

Anthoni PM, Unsworth MH, Law BE *et al*. (2002) Seasonal differences in C and water vapor exchange in young and old-growth ponderosa pine forest. *Agricultural and Forest Meteorology*, **111**, 202–222.

Baldocchi DD (2003) Assessing the eddy covariance technique for evaluating C exchange rates of ecosystems: past, present and future. *Global Change Biology*, **9**, 479–492.

Baldocchi DD, Falge E, Gu L *et al*. (2001) FLUXNET: a new tool to study the temporal and spatial variability of ecosystem-scale C dioxide, water vapor, and energy flux densities. *Bulletin of the American Meteorology Society*, **82**, 2415–2434.

Barford CC, Wofsy SW, Goulden ML *et al*. (2001) Factors controlling long- and short-term sequestration of atmospheric CO_2 in a mid-latitude forest. *Science*, **294**, 1688–1691.

Barr AG, Black TA, Hogg EH *et al*. (2004) Inter-annual variability in the leaf area index of a boreal aspen-hazelnut forest in relation to net ecosystem production. *Agricultural and Forest Meteorology*, **126**, 237–255.

Black TA, Gaumont-Guay D, Jassal RS *et al*. (2004) Measurement of C dioxide exchange between the boreal forest and the atmosphere. In: *C Balance of Forest Biomes* (eds Griffiths H, Jarvis P), pp. 151–186. BIOS Scientific Publishers, UK.

Bond-Lamberty B, Wang C, Gower ST (2004a) Contribution of root respiration to soil surface CO_2 flux in a boreal black spruce chronosequence. *Tree Physiology*, **24**, 1387–1395.

Bond-Lamberty B, Wang C, Gower ST (2004b) A global relationship between the heterotrophic and autotrophic components of soil respiration? *Global Change Biology*, **10**, 1756–1766.

Bond-Lamberty B, Wang C, Gower ST (2004c) Net primary production and net ecosystem production of a boreal black spruce wildfire chronosequence. *Global Change Biology*, **10**, 473–487.

Chen J, Falk M, Euskirchen E *et al*. (2002) Biophysical controls of C flows in three successional Douglas-fir stands based on eddy-covariance measurements. *Tree Physiology*, **22**, 169–177.

Chen J, Franklin JF, Spies TA (1993) Contrasting microclimate patterns among clearcut, edge, and interior area of old-growth Douglas-fir forest. *Agricultural and Forest Meteorology*, **63**, 219–237.

Chen J, Paw U KT, Ustin SL *et al*. (2004) Net ecosystem exchanges of C, water, and energy in young and old-growth Douglas-Fir forests. *Ecosystems*, **7**, 534–544.

Coble DW, Milner KS, Marshall JD (2001) Above- and below-ground production of trees and other vegetation on contrasting aspects in western Montana: a case study. *Forest Ecology and Management*, **142**, 231–241.

© 2007 The Authors

Drewitt GB, Black TA, Nesic Z *et al*. (2002) Measuring forest floor CO_2 fluxes in a Douglas-fir forest. *Agricultural and Forest Meteorology*, **110**, 299–317.

Efron B, Tibshirani RJ (1998) *An Introduction to the Bootstrap*. Chapman & Hall/CRC, Boca Raton.

Falge E, Baldocchi D, Tenhunen J *et al*. (2002) Seasonality of ecosystem respiration and gross primary production as derived from FLUXNET measurements. *Agricultural and Forest Meteorology*, **113**, 53–74.

Field CB, Kaduk J (2004) The C balance of an old-growth forest: building across approaches. *Ecosystems*, **7**, 525–533.

Gifford RM (1994) The global C cycle: a viewpoint on the missing sink. *Australian Journal of Plant Physiology*, **21**, 1–15.

Gifford RM (2003) Plant respiration in productivity models: conceptualisation, representation and issues for global terrestrial carbon-cycle research. *Functional Plant Biology*, **30**, 171–186.

Goetz SJ, Prince SD (1999) Modelling terrestrial C exchange and storage: evidence and implications of functional convergence in light-use efficiency. *Advances in Ecological Research*, **28**, 57–92.

Gower ST, McMurtrie RE, Murty D (1996) Aboveground net primary production decline with stand age: potential causes. *Trends in Ecology & Evolution*, **11**, 378–382.

Griffis TJ, Black TA, Gaumont-Guay D *et al*. (2004) Seasonal variation and partitioning of ecosystem respiration in a southern boreal aspen forest. *Agricultural and Forest Meteorology*, **125**, 207–223.

Griffiths RP, Swanson AK (2001) Forest soil characteristics in a chronosequence of harvested Douglas-fir forests. *Canadian Journal of Forest Research*, **31**, 1871–1879.

Harmon ME, Bible K, Ryan MG *et al*. (2004) Production, respiration, and overall C balance in an old-growth *Pseudotsuga–Tsuga* forest ecosystem. *Ecosystems*, **7**, 498–512.

Howard EA, Gower ST, Foley JA *et al*. (2004) Effects of logging on C dynamics of a jack pine forest in Saskatchewan, Canada. *Global Change Biology*, **10**, 1267–1284.

Humphreys ER (2004) *Net ecosystem production of three coastal Douglas-fir stands at different stages of development after harvesting*. PhD Thesis, University of British Columbia, Vancouver, 122 pp.

Humphreys ER, Black TA, Ethier GJ *et al*. (2003) Annual and seasonal variability of sensible and latent heat fluxes above a coastal Douglas-fir forest, British Columbia, Canada. *Agricultural and Forest Meteorology*, **115**, 109–125.

Humphreys ER, Black TA, Morgenstern K *et al*. (2005) Net ecosystem production of a Douglas-fir stand for three years following clearcut harvesting. *Global Change Biology*, **11**, 450–464.

Humphreys ER, Black TA, Morgenstern K *et al*. (2006) Carbon dioxide fluxes in three coastal Douglas-fir stands at different stages of development after harvesting. *Agricultural and Forest Meteorology*, doi: 10.1016/j.agrformet.2006.03.018.

Janisch JE, Harmon ME (2002) Successional changes in live and dead wood C stores: implications for net ecosystem productivity. *Tree Physiology*, **22**, 77–89.

Janssens IA, Lankreijer H, Matteucci G *et al*. (2001) Productivity overshadows temperature in determining soil and ecosystem respiration across European forests. *Global Change Biology*, **7**, 269–278.

Jolly WM, Nemani R, Running SW (2005) A generalized, bioclimatic index to predict foliar phenology in response to climate. *Global Change Biology*, **11**, 619–632.

Kolari P, Pumpanen J, Rannik Ü *et al*. (2004) Carbon balance of different aged Scots pine forests in Southern Finland. *Global Change Biology*, **10**, 1106–1119.

Kowalski AS, Loustau D, Berbigier P *et al*. (2004) Paired comparisons of C exchange between undisturbed and regenerating stands in four managed forests in Europe. *Global Change Biology*, **10**, 1707–1723.

Lavigne MB, Ryan MG, Anderson DE *et al*. (1997) Comparing nocturnal eddy covariance measurements to estimates of ecosystem respiration made by scaling chamber measurements. *Journal of Geophysical Research*, **102**, 28977–28985.

Law BE, Falge E, Baldocchi DD *et al*. (2002) Environmental controls over C dioxide and water vapor exchange of terrestrial vegetation. *Agricultural and Forest Meteorology*, **113**, 97–120.

Law BE, Sun OJ, Campbell J *et al*. (2003) Changes in C storage and fluxes in a chronosequence of ponderosa pine. *Global Change Biology*, **9**, 510–524.

Litvak M, Miller S, Wofsy SC *et al*. (2003) Effect of stand age on whole ecosystem CO_2 exchange in the Canadian boreal forest. *Journal of Geophysical Research*, **108**, 8225.

Lo E (2005) Gaussian error propagation applied to ecological data: post-ice-storm-downed woody biomass. *Ecological Monographs*, **75**, 451–466.

MacKinnon A (2003) West coast, temperate, old-growth forests. *Forest Chronicle*, **79**, 475–484.

Mitchell KJ, Stone M, Grout SE *et al*. (2000) *TIPSY Version 3.0*. Ministry of Forests, Research Branch, Victoria, BC.

Moncrieff J, Malhi Y, Leuning R (1996) The propagation of errors in long-term measurements of land atmosphere fluxes of C and water. *Global Change Biology*, **2**, 231–240.

Morgenstern K, Black TA, Humphreys ER *et al*. (2004) Sensitivity and uncertainty of the C balance of a Pacific Northwest Douglas-fir forest during an El Niño/La Niña cycle. *Agricultural and Forest Meteorology*, **123**, 210–219.

Mund M, Kummetz E, Hein M *et al*. (2002) Growth and C stocks of a spruce forest chronosequence in central Europe. *Forest Ecology and Management*, **171**, 275–296.

Niinemets Ü (2002) Stomatal conductance alone does not explain the decline in foliar photosynthetic rates with increasing tree age and size in *Picea abies* and *Pinus sylvestris*. *Tree Physiology*, **22**, 515–535.

Pojar J, Klinka K, Demarchi DA (1991) Coastal Douglas-fir zone. In: *Ecosystems of British Columbia* (eds Meidinger DV, Pojar J), pp. 81–93. British Columbia Ministry of Forests, Research Branch, Victoria, BC.

Pregitzer KS, Euskirchen ES (2004) C cycling and storage in world forests: biome patterns related to forest age. *Global Change Biology*, **10**, 2052–2077.

Röser C, Montagnani L, Schulze ED (2002) Net CO_2 exchange rates in three different successional stages of the ''Dark Taiga'' of central Siberia. *Tellus B*, **54**, 642–654.

Ryan MG, Binkley D, Fownes JH *et al*. (2004) An experimental test of the causes of forest growth decline with stand age. *Ecological Monographs*, **74**, 393–414.

© 2007 The Authors

Ryan MG, Lavigne MB, Gower ST (1997) Annual carbon cost of autotrophic respiration in boreal forest ecosystems in relation to species and climate. *Journal of Geophysical Research*, **102**, 28871–28883.

Schwalm CR, Black TA, Morgenstern K *et al*. (2005) *Temperature effects along a Coastal Douglas-fir chronosequence*. Presented at the 2005 FLUXNET Canada Annual General Meeting in Quebec, QC, Canada

Shirke PA (2001) Leaf photosynthesis, dark respiration and florescence as influenced by leaf age in an evergreen tree, *Prosopis juliflora*. *Photosynthetica*, **39**, 305–311.

Simpson W, TenWolde A (1999) Physical properties and moisture relations of wood. In: *Wood Handbook – Wood as an Engineering Material*. *FPL-GTR-113* pp. 3-1–3-24. U.S. Department of Agriculture, Forest Service, Forest Products Laboratory, Madison, WI.

Spittlehouse D (2003) Water availability, climate change and the growth of Douglas-fir in the Georgia Basin. *Canadian Water Resources Journal*, **20**, 673–688.

Thuille A, Buchmann N, Schulze ED (2000) C stocks and soil respiration rates during deforestation, grassland use and subsequent Norway spruce afforestation in the Southern Alps, Italy. *Tree Physiology*, **20**, 849–857.

Vose JM, Ryan MG (2002) Seasonal respiration of foliage, fine roots, and woody tissues in relation to growth, tissue N, and photosynthesis. *Global Change Biology*, **8**, 182–193.

Waring RH, Landsberg JJ, Williams M (1998) Net primary production of forests: a constant fraction of gross primary production? *Tree Physiology*, **18**, 129–134.

Waring RH, Schlesinger WH (1985) *Forest Ecosystems: Concepts and Management*. Academic Press, Inc, Orlando, FL.

Wesely ML, Hart RL (1985) Variability of short term eddy-correlation estimates of mass exchange. In: *The Forest – Atmosphere Interaction* (eds Hutchinson BA, Hicks BB), pp. 591–612. D. Reidel, Dordrecht.

Williams M, Schwarz PA, Law BE *et al*. (2005) An improved analysis of forest carbon dynamics using data assimilation. *Global Change Biology*, **11**, 89–105.

© 2007 The Authors